High-dimensional orbital angular momentum entanglement concentration based on Laguerre–Gaussian mode selection

2013 Laser Phys. Lett. 10 095201

(http://iopscience.iop.org/1612-202X/10/9/095201)

IOP PUBLISHING LASER PHYSICS LETTERS
Laser Phys. Lett. **10** (2013) 095201 (5pp) doi:10.1088/1612-2011/10/9/095201

LETTER

High-dimensional orbital angular momentum entanglement concentration based on Laguerre–Gaussian mode selection

Wuhong Zhang[1], Ming Su[1], Ziwen Wu, Meng Lu, Bingwei Huang and Lixiang Chen

Department of Physics and Laboratory of Nanoscale Condensed Matter Physics, Xiamen University, Xiamen 361005, People's Republic of China

E-mail: chenlx@xmu.edu.cn

Received 15 May 2013
Accepted for publication 27 May 2013
Published 22 July 2013
Online at stacks.iop.org/LPL/10/095201

Abstract
Twisted photons enable the definition of a Hilbert space beyond two dimensions by orbital angular momentum (OAM) eigenstates. Here we propose a feasible entanglement concentration experiment, to enhance the quality of high-dimensional entanglement shared by twisted photon pairs. Our approach is started from the full characterization of entangled spiral bandwidth, and is then based on the careful selection of the Laguerre–Gaussian (LG) modes with specific radial and azimuthal indices p and ℓ. In particular, we demonstrate the possibility of high-dimensional entanglement concentration residing in the OAM subspace of up to 21 dimensions. By means of LabVIEW simulations with spatial light modulators, we show that the Shannon dimensionality could be employed to quantify the quality of the present concentration. Our scheme holds promise in quantum information applications defined in high-dimensional Hilbert space.

(Some figures may appear in colour only in the online journal)

1. Introduction

Recently, there has been much research attention focused on twisted photons as well as their applications in both classical and quantum regimes [1]. Twisted photons are so named because of their characteristic helical wavefronts of $\exp(i\ell\phi)$, where ϕ is the azimuthal angle and ℓ is an integer. A single photon bearing such a helical wavefront is in its orbital angular momentum (OAM) eigenstate $|\ell\rangle$ and carries an OAM of $\ell\hbar$ [2]. The significance of twisted photons lies in the potential of encoding qudits (quantum state in d dimensions), since $|\ell\rangle$ forms an infinite-dimensional, complete set of orthogonal modes [3]. This is obviously in contrast with the two-dimensional thinking regarding photon spin associated with the polarization of light. Thus it provides a promising playground for exploring further features of quantum mechanics with twisted photons [4].

As is well known, most quantum protocols, such as quantum teleportation [5] and quantum key distribution [6], rely on the maximally entangled states to function well. However, the nonmaximally entangled states are most common in practice. Spontaneous parametric down-conversion (SPDC) is a reliable source for generating photon pairs that are well entangled in their spatial degree of OAM [7]. This entangled

[1] These authors contributed equally to this work.

OAM spectrum is high-dimensional but inevitably of limited spiral bandwidth; namely, photon pairs with a smaller OAM are more frequent than the higher-order ones, and therefore result in a nonmaximally entangled state [8]. For this reason, some 'procrustean' methods were reported to extract the maximal entanglement [9]. Vaziri *et al* concentrated a maximally entangled OAM qutrit by means of optimal lens configurations [10]. Also, Data *et al* demonstrated the OAM entanglement concentration in a much higher dimension with the use of a spatial light modulator [11]. We further show that such concentration can be performed in arbitrary OAM subspaces [12]. Also, we propose a hyperconcentration scheme to maximize the entanglement in the composite spin–orbit space [13]. Here we propose another efficient scheme to concentrate the maximally entangled OAM qudits. Our approach starts from the full characterization of entangled spiral bandwidth, and is based on the careful selection of the LG modes, where the radial index p of LG modes is taken into account to effectively equalize the OAM modes in the entangled spiral spectrum. The scheme is very straightforward and feasible with current experimental techniques. From the applied point of view, there are several advantages when using high-dimensional maximally entangled systems, such as higher information-density coding and greater resilience to errors, increased level of security, simplification of quantum logic, and closing the detection loophole in Bell experiments [14–17]. Therefore we anticipate that our method has potential applications in quantum information processing with entangled qudits.

2. Theory and application of high-dimensional OAM entanglement concentration

Entanglement of OAM arises from phase matching in a down-converted crystal. As shown in our proposed scheme in figure 1, the down-converted crystal is a BBO cut for type-I SPDC, where one pump ultraviolet photon is split collinearly into two degenerate ones with the same polarization. The signal and idler photons are separated by a non-polarizing beam splitter (BS), and manipulated with spatial light modulators (SLMs), respectively. A set of lenses (not shown) images the SLMs onto single-mode fibers (SMFs), which therefore inversely measure the specific OAM superposed states defined by the SLMs. The output of single-photon detectors connected to the SMFs is finally fed to a coincidence counting circuit (&).

In a more general picture, the spatial structure of down-converted biphotons should be expressed in terms of LG_p^ℓ modes $|\ell, p\rangle$, where ℓ and p are the azimuthal and radial indices, respectively. As shown by Yao and Miatto *et al* [18, 19], the biphoton state can be written as

$$|\Psi\rangle_{\mathrm{SPDC}} = \sum_{\ell,p_s}\sum_{\ell,p_i} C_{p_s,p_i}^{\ell_s,\ell_i}|\ell_s, p_s\rangle|\ell_i, p_i\rangle, \qquad (1)$$

where $|C_{p_i,p_s}^{\ell_i,\ell_s}|^2$ denotes the joint probability for finding one signal photon in the mode $|\ell_s, p_s\rangle$ and one idler photon in $|\ell_i, p_i\rangle$. For a fundamental Gaussian pump with zero OAM, the conservation law of angular momentum ensures that $\ell_s + \ell_i = 0$. The ratios of the beam waist of the pump to that of the signal and idler are denoted as γ_s and γ_i, respectively. In an actual experiment it is not possible to use a pump with an arbitrarily large beam waist due to the finite crystal size. It is also not possible to shrink the size of the signal and idler enough. Therefore we usually have $\gamma_s = \gamma_i = 1$. Equation (20) in [19] describing the complex amplitude can thus be simplified as

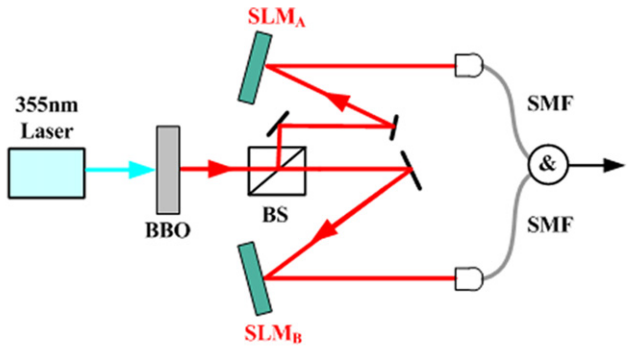

Figure 1. Proposed experimental scheme.

$$C_{p_s,p_i}^{\ell,-\ell} \propto \frac{K_{p_s,p_i}^{|\ell|}(-2)^{|\ell|}}{3^{p_s+p_i+|\ell|}} \times {}_2F_1\left[\begin{matrix}-p_i, p_s \\ -p_i - p_s - |\ell|\end{matrix}; 5\right], \qquad (2)$$

where $K_{p_i,p_s}^{|\ell|} = \frac{(p_i+p_s+|\ell|)!}{\sqrt{p_i!p_s!(p_s+|\ell|)!(p_i+|\ell|)!}}$, and ${}_2F_1$ is the Gauss hypergeometric function. As can be seen, the complex amplitude $C_{p_s,p_i}^{\ell,-\ell}$ is generally not only as an even function of ℓ, but also modulated by p_s and p_i. A case we commonly encounter is that which considers only $p_s = p_i = 0$, namely, $|C_{0,0}^{\ell,-\ell}| = (\frac{2}{3})^{|\ell|}$, as is visualized by the inset of figure 3(a). The limited nature of this spiral bandwidth (with ℓ ranging from -10 to $+10$) indicates the low quality of the associated 21-dimensional entanglement. The aim of entanglement concentration is to modulate and convert these nonequal relative amplitudes into equal ones, and therefore obtain the maximally entangled state. Previous studies consider only the eigenstate $|\ell\rangle$ with $p_s = p_i = 0$ or averaged over all p values, and concentration is then performed by changing the coupling efficiency of the lens [10] or modulating the mode weight of the diffractive gratings [11, 12]. In contrast, if we take the radial indices p into consideration, then it is possible to find specific pairs of p_s and p_i to equalize $|C_{p_s,p_i}^{\ell,-\ell}|$ straightforwardly for different OAM numbers ℓ. A simple example with $|\ell| \leq 3$ is shown in figures 2(a)–(d) to illustrate the optimal procedure. The numerical calculations based on equation (2) find that for $|\ell| < 4$ the overall complex amplitude $|C_{p_s,p_i}^{\ell,-\ell}|$ decreases as $|\ell|$ increases for a given pair of p_s and p_i. Also, for a fixed ℓ, the peak of $|C_{p_s,p_i}^{\ell,-\ell}|$ is centered around $p_s = p_i = 0$. Based on this scenario, we first find out the maximal value of $|C_{0,0}^{3,-3}|$ in figure 2(d). Then we sweep each of figures 2(a)–(c) to select a pair of p_s and p_i, whose value most closely equals or approaches $|C_{0,0}^{3,-3}|$. Along this line, the desired LG modes we select are $\mathrm{LG}_{4,4}^{0,0}$, $\mathrm{LG}_{2,2}^{1,-1}$, $\mathrm{LG}_{1,1}^{2,-2}$ and $\mathrm{LG}_{0,0}^{3,-3}$, as shown in figure 2. After considering the symmetry of $|\ell|$, we finally have a seven-dimensional maximally entangled state as

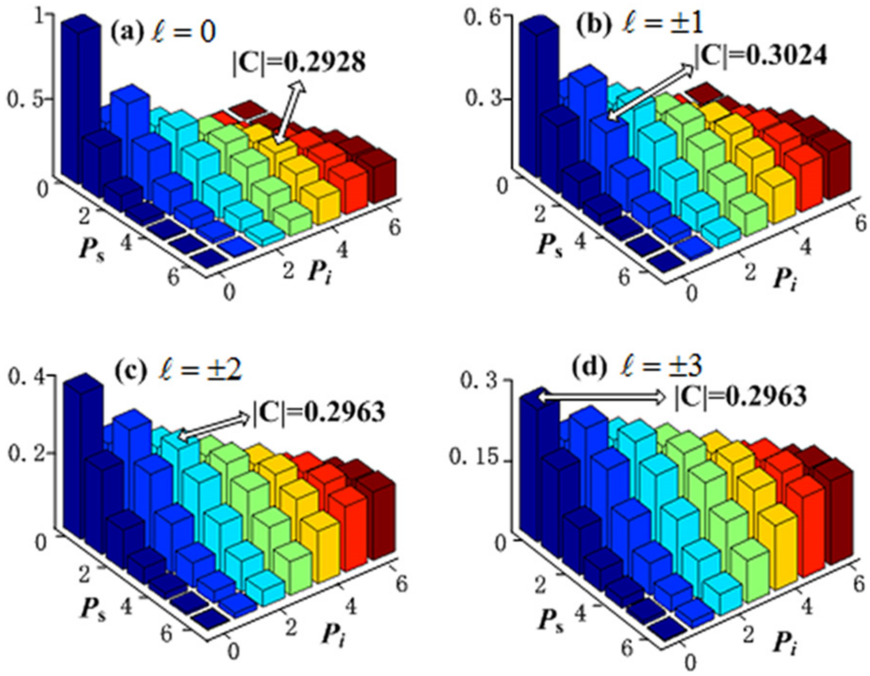

Figure 2. Numerical illustration of $|C^{\ell,-\ell}_{p_s,p_i}|$ on ℓ, p_i, p_s, and the optimal selection of desired LG modes.

Table 1. The desired LG modes for 21-dimensional OAM entanglement concentration.

l	0	1	2	3	4	5	6	7	8	9	10
p_i	4	5	9	1	7	9	1	7	3	12	14
p_s	1	9	5	4	11	14	3	10	4	14	14

follows:

$$\begin{aligned} |\psi_7\rangle = {} & 0.2963|-3,0;+3,0\rangle + 0.2963|-2,2;+2,2\rangle \\ & + 0.3036|-1,3;+1,3\rangle + 0.2928|0,4;0,4\rangle \\ & + 0.3036|+1,3;-1,3\rangle + 0.2963|+2,2;-2,2\rangle \\ & + 0.2963|+3,0;-3,0\rangle. \end{aligned} \tag{3}$$

In principle, our scheme is able to perform any entanglement concentration residing in an arbitrary-dimensional OAM subspace. Another example up to 21 dimensions is demonstrated, where ℓ ranges from -10 to $+10$. The optimal procedure for LG mode selection is similar to that in figure 2. Surprisingly, the LG mode we first select for $\ell = +10$ is $\mathrm{LG}^{10,-10}_{14,14}$ rather than $\mathrm{LG}^{10,-10}_{0,0}$, and $|C^{10,-10}_{14,14}| \approx 0.0722$ compared with $|C^{10,-10}_{0,0}| \approx 0.0173$. This is because for different ℓ ranges, the dependence on the p index exhibits a more complex behavior. If $|\ell| \le 4$, then the probability decreases monotonously as p increases, as previously mentioned. In contrast, if $|\ell| \ge 5$ the probability increases first and then decreases along with p. Therefore for $\ell = +10$, it is found that the maximal probability is achieved with $p_s = p_i = 14$. After a lengthy but straightforward numeric search, the desired LG modes we select are listed in table 1. The modes for minus ℓ are not shown owing to the SPDC symmetry of $C^{-\ell,\ell}_{p_s,p_i} = C^{\ell,-\ell}_{p_s,p_i}$. Therefore after taking p_s and p_i into account, the limited entangled spiral spectrum, as shown by the inset of figure 3(a), can now be successfully flattened and converted into a comblike maximally entangled one, as shown by the inset of figure 3(b).

3. Shannon dimensionality after entanglement concentration

After concentration, it is crucial to quantify the quality of entanglement. Here we adopt the concept of Shannon dimensionality to characterize the effective size of the involved Hilbert space [20–24]. For maximal entanglement, it has been proved that the Shannon dimensionality is just equivalent to the Schmidt number [12, 13]. Thus the larger the Shannon dimensionality, the higher the degree of entanglement [25]. To obtain the Shannon dimensionality, it is essential to impart a relative rotation of $\Delta\alpha = \alpha_s - \alpha_i$ to the measured holograms in the signal and idler arms, respectively. Based on LabVIEW simulations, we have illustrated in figures 4(a)–(f) the desired holograms, intensity and phase patterns displayed in the SLMs for the 21 OAM mode superpositions, respectively. Such a rotation of the measured holograms just brings a phase shift $\exp(\mathrm{i}\ell\phi)$ to each OAM mode so that equation (1) is modified as

$$|\Psi\rangle = \sum_l \exp(\mathrm{i}\ell\Delta\alpha) C^{l,-l}_{p_s,p_i} |l, p_s; -l, p_i\rangle. \tag{4}$$

Then the coincidence count is given by $P(\Delta\alpha) = |\sum_l C^{l,-l}_{p_s,p_i} \exp(\mathrm{i}\ell\Delta\alpha)|^2$, and the Shannon dimensionality can be deduced from the peak-normalized count, $P(\Delta\alpha)/P_{\max}$, that is, $D = 2\pi P_{\max} / \int_0^{2\pi} P(\Delta\alpha)\,\mathrm{d}\Delta\alpha$. Based on LabVIEW simulations, we have also plotted in figures 3(a) and (b)

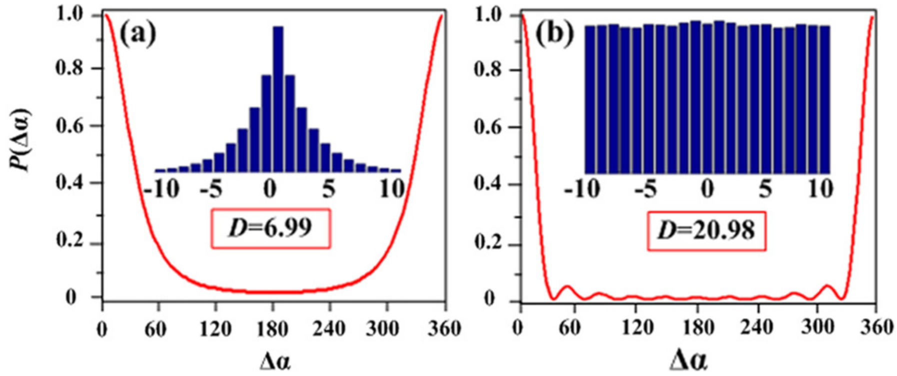

Figure 3. Shannon dimensionality calculations for (a) limited spiral spectrum with $p_s = p_i = 0$ and (b) comblike spiral spectrum with careful selection of p_s and p_i.

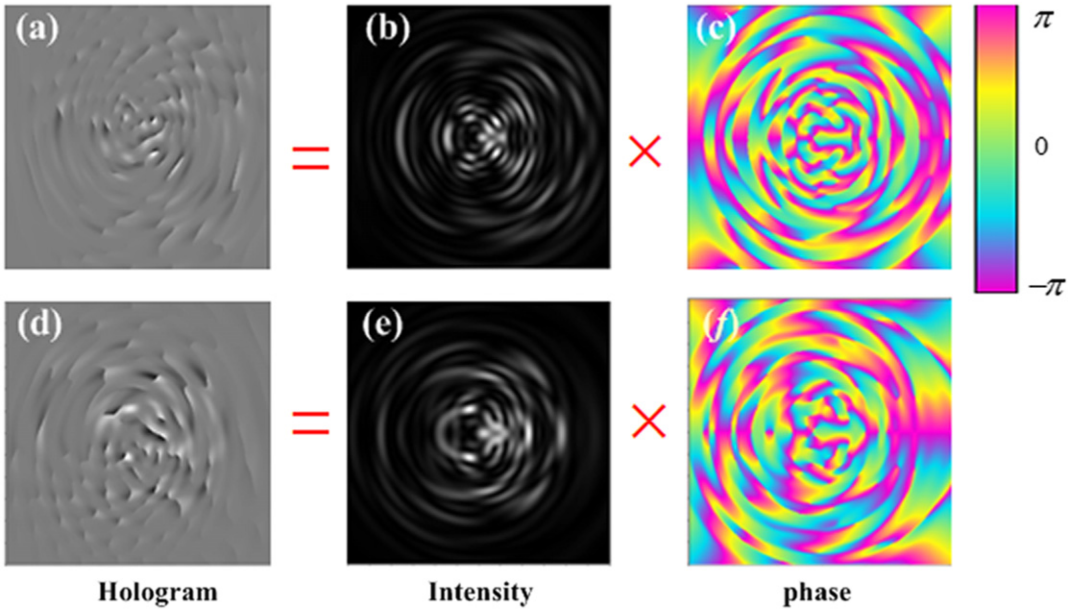

Figure 4. The desired hologram ((a), (d)), intensity ((b), (e)), and phase patterns ((c), (f)) displayed in the signal and idler SLMs required for 21-dimensional concentration.

two coincidence curves for the cases before and after entanglement concentration, respectively. As can be seen, the Shannon dimensionality is significantly improved after concentration, up to $D = 20.98$, by comparison with that of $D = 6.99$ without careful LG mode selection.

4. Conclusion

To conclude, we have demonstrated the possibility of high-dimensional entanglement concentration shared by twisted photon pairs, by means of the careful selection of LG modes with specific ℓ and p indices. Furthermore, we have shown that the Shannon dimensionality is a good quantifier for the present entanglement concentration. Our scheme is very straightforward and feasible with current experimental techniques. It is noted that the goal of any entanglement concentration is to equalize the OAM modes in the entangled spiral spectrum such that it is able to cut off or discard the extra probability of the larger terms in equation (1). In other words, it sacrifices the quantity of initial photon pairs to enhance the quality of the final entangled state. Therefore the advantage of our method, namely, the probability that a given input pair survives the LG mode selection, is directly linked to each $|C^{\ell,-\ell}_{p_s,p_i}|^2$. We can estimate that in our case the yield of output maximally entangled pairs is given by $\eta = \sum_{\ell=-N}^{+N} |C^{\ell,-\ell}_{p_s,p_i}|^2 \approx (2N+1)|C^{N,-N}_{p'_s,p'_i}|^2$, where $|C^{N,-N}_{p'_s,p'_i}| = \max\{|C^{N,-N}_{p_s,p_i}|\}$. Further, when compared with other schemes considering $|\ell\rangle$ with only $p = 0$ [10–12], our scheme would improve the efficiency by a factor of $\kappa = |C^{N,-N}_{p'_s,p'_i}/C^{N,-N}_{0,0}|^2$, for example $N = 10$ gives $\kappa \approx 17.4$, as mentioned above. We anticipate that our scheme holds promise for use in some quantum information applications defined in high-dimensional Hilbert space.

Acknowledgments

We thank the Optics Group at the University of Glasgow for kind help in the LabVIEW. This work is supported by the National Natural Science Foundation of China (NSFC) (grant 11104233), the Fundamental Research Funds for the Central Universities (grant 2011121043 and 2012121015), and the Natural Science Foundation of Fujian Province of China (Grant 2011J05010 and 2012J01285).

References

[1] Yao A M and Padgett M J 2011 *Adv. Opt. Photon.* **3** 161–204
[2] Allen L, Beijersbergen M W, Spreeuw R J C and Woerdman J P 1992 *Phys. Rev.* A **45** 8185
[3] Molina-Terriza G, Torres J P and Torner L 2002 *Phys. Rev. Lett.* **88** 013601
[4] Molina-Terriza G, Torres J and Torner L 2007 *Nature Phys.* **3** 305–10
[5] Bennett C H, Brassard G, Crepeau C, Jozsa R, Peres A and Wootters W 1993 *Phys. Rev. Lett.* **70** 1895
[6] Groblacher S, Jennewein T, Vaziri A, Weihs G and Zeilinger A 2006 *New J. Phys.* **8** 75
[7] Mair A, Vaziri A, Weihs G and Zeilinger A 2001 *Nature* **412** 313
[8] Torres J P, Alexandrescu A and Torner L 2003 *Phys. Rev.* A **68** 050301(R)
[9] Bennett C H, Bernstein H J, Popescu S and Schumacher B 1996 *Phys. Rev.* A **53** 2046
[10] Vaziri A, Pan J W, Jennewein T, Weihs G and Zeilinger A 2003 *Phys. Rev. Lett.* **91** 227902
[11] Dada A C, Leach J, Buller G S, Padgett M J and Andersson E 2011 *Nature Phys.* **7** 677
[12] Chen L and Wu Q 2012 *Laser Phys. Lett.* **9** 759–64
[13] Chen L 2012 *Phys. Rev.* A **85** 012311
[14] Bruss D 1998 *Phys. Rev. Lett.* **81** 3018
[15] Bechmann-Pasquinucci H and Peres A 2000 *Phys. Rev. Lett.* **85** 3313
[16] Lanyon B P, Barbieri M, Almeida M P, Jennewein T, Ralph T C, Resch K J, Pryde G J, OBrien J L, Gilchrist A and White A G 2009 *Nature Phys.* **5** 134–40
[17] Vrtesi T, Pironio S and Brunner N 2010 *Phys. Rev. Lett.* **104** 060401
[18] Yao A M 2011 *New J. Phys.* **13** 053048
[19] Miatto F M, Yao A M and Barnett S M 2011 *Phys. Rev.* A **83** 033816
[20] Pors J B, Oemrawsingh S S R, Aiello A, van Exter M P, Eliel E R, Hooft G W 't and Woerdman J P 2008 *Phys. Rev. Lett.* **101** 120502
[21] Chen L and She W 2009 *Opt. Lett.* **34** 1855
[22] Chen L, Leach J, Jack B, Padgett M J, Franke-Arnold S and She W 2010 *Phys. Rev.* A **82** 033822
[23] Pors J B, Miatto F, 't Hooft G W, Eliel E R and Woerdman J P 2011 *J. Opt.* **13** 064008
[24] Giovannini D, Miatto F M, Romero J, Barnett S M, Woerdman J P and Padgett M J 2012 *New J. Phys.* **14** 073046
[25] Law C K and Eberly J H 2004 *Phys. Rev. Lett.* **92** 127903